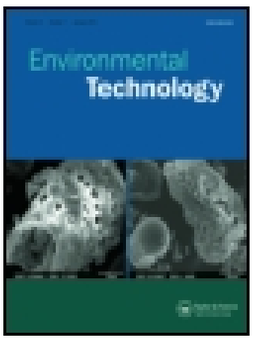

Environmental Technology

ISSN: 0959-3330 (Print) 1479-487X (Online) Journal homepage: https://www.tandfonline.com/loi/tent20

A novel amperometric biosensor for rapid detection of ethanol utilizing gold nanoparticles and enzyme coupled PVC reaction cell

Vinita Hooda, Anjum Gahlaut & Vikas Hooda

To cite this article: Vinita Hooda, Anjum Gahlaut & Vikas Hooda (2020): A novel amperometric biosensor for rapid detection of ethanol utilizing gold nanoparticles and enzyme coupled PVC reaction cell, Environmental Technology, DOI: 10.1080/09593330.2020.1726472

To link to this article: https://doi.org/10.1080/09593330.2020.1726472

Accepted author version posted online: 04 Feb 2020.

Publisher: Taylor & Francis & Informa UK Limited, trading as Taylor & Francis Group

Journal: *Environmental Technology*

DOI: 10.1080/09593330.2020.1726472

A novel amperometric biosensor for rapid detection of ethanol utilizing gold nanoparticles and enzyme coupled PVC reaction cell

Vinita Hooda, Anjum Gahlaut and Vikas Hooda*

Centre for Biotechnology, Maharshi Dayanand University, Rohtak -124001, Haryana

*** Corresponding Author**

Dr. Vikas Hooda

Assistant Professor

Centre for Biotechnology,

M. D. University, Rohtak, Haryana, India

Tel: +911262393113; +918295558888

E-mail: advance.biotech@gmail.com

Abstract

The research was aimed at the fabrication of an improved enzyme based amperometric biosensor for rapid quantification of ethanol. Alcohol oxidase (AOX) from *Pichia pastoris* was covalently immobilized on chemically treated polyvinylchloride (PVC) beaker and subsequently horseradish peroxidase (HRP), nafion (Nf), carboxylated multi-walled carbon nanotubes (c-MWCNTs), chitosan (CHIT) and gold nanoparticles (AuNPs) were immobilized onto Au electrode to fabricate a working electrode. The enzyme coated PVC surface was analyzed morphologically via scanning electron microscopy (SEM). At different stages of construction, the electrochemical properties of working electrode were deciphered by cyclic voltammetry (CV) and electrochemical impedance

spectroscopy (EIS). The biosensor displayed optimal response in a short time span of 12 s at pH 7.5 and 35 ˚C temperature. The working range exhibited by the proposed biosensor was 0.01 mM-42 mM with a limit of detection (LOD) of 0.0001 µM and storage stability of 180 days at 4˚ C. When level of alcohol was evaluated in commercial samples via standard assay kit and existing biosensor, a good correlation ($R^2 = 0.98$) was observed which authenticates its reliability.

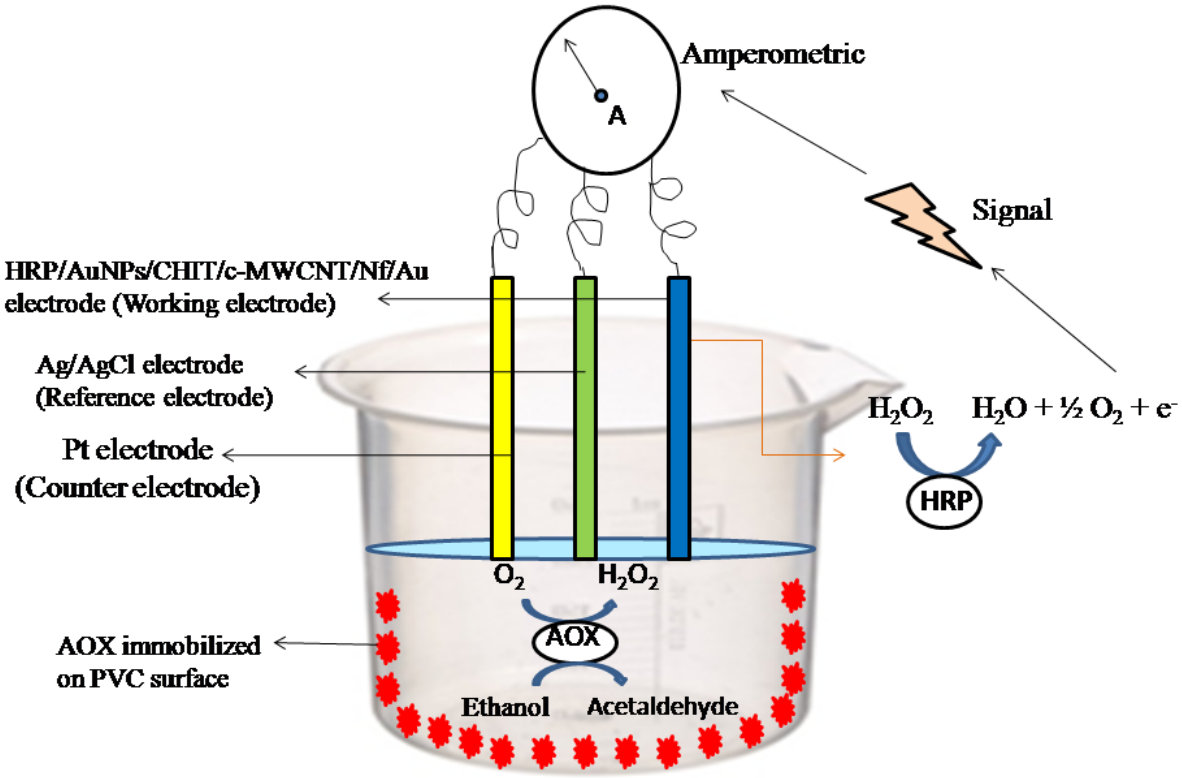

Keywords: Ethanol, Biosensor, Alcohol oxidase, HRP, PVC

Introduction

It is enormously imperative to quantify the levels of alcohol in fermentation processes, food industries, body fluids analysis (serum, blood, saliva, urine) and medicine industries due to its psychological and toxicological effects [1]. The quality of alcoholic beverages (spirits, liquor, beer, wine), food and pulp should be controlled via steadfast analytical methods for determination of ethanol [2]. A number of conventional procedures are available for detection of ethanol such as refractrometry, colorimetry, redox titrations, chromatography and spectroscopic techniques. These

approaches are cumbersome, expensive, time-consuming and complex in performing; alternatively, biosensors are inevitable. Enzyme based biosensing methods overcome these shortcomings and offer efficient catalytic properties, brilliant specificity, reliability, sensitivity, low cost of fabrication as well as quick and on line availability for the quantification of ethanol [3]. Amperometric biosensors for sensing of ethanol involve two chief enzymes- alcohol oxidase [4] and alcohol dehydrogenase (ADH) [5]. In case of biosensors based on ADH, the enzyme catalyzes the oxidation of ethanol to acetaldehyde in presence of NAD^+ which further gets reduced to NADH. The release of electrons and protons oxidize this NADH and consequently monitored amperometricaly [6]. These sensors have limited operational stability and nuisance of continuous requirement of coenzyme NAD^+ in the assay which increases the manufacturing cost [7]. On the other hand, AOX (EC 1.1.3.13) based sensors are undemanding as molecular oxygen is the only requirement for the oxidation of alcohol into corresponding aldehyde and simultaneously H_2O_2 is released, devoid of using any additional cofactor [8]. The bio-recognition system involving AOX has credit of some advantages such as occurrence of tightly bound flavin-based cofactor at redox center of enzyme and irreversible nature of catalytic reaction [1]. AOX utilizes oxygen as natural electron acceptor thus liberating H_2O_2. Numerous electrochemical biosensors have been reported which utililize alcohol oxidase for the detection of alcohol [9]. These sensors involved immobilization of AOX either on MWCNTs modified glassy carbon electrode [10], conducting polymers such as 4,7-dithien-2-yl-2,1,3-benzothiadiazole and 3,4-ethylenedioxythiophene [11], membrane like eggshell membrane [12], nafion membrane [13-14] and poly(vinyl alcohol) membrane [15], graphite epoxy composite electrode (GECE) [16] or graphite powder/an epoxy resin bicomposite electrode [17]. The membrane immobilized enzymes have benefit of reusability and stability when compared with sensors utilizing electrodeposited layer which show fast response and ultrasensitivity. PVC has achieved notable interest to fabricate a reaction beaker with enzyme immobilized inside it that functions as electrochemical cell for analyte determination [18-21]. Taking account of various astonishing characteristics of PVC including chemical inertness, corrosion resistance, weather resistance, high strength-to-weight ratio, easy availability, light weight, cost-effectiveness and toughness [19], we described AOX immobilization on surface of conducting and non-fragile PVC. The deployment of PVC in bioanalysis will expose novel innovations in area of allied biomedical instruments, designing and fabricating biosensors as well as diagnostic kits.

Over the past few years, the use of nanoparticles in development of next generation sensors has been augmented credited to their exceptional electrical, optical, thermal and mechanical properties which help to ameliorate vital performance indexes- selectivity, sensitivity, repeatability and stability. c-MWCNTs display high electroactive surface owing to its excellent thermal and electrical conductivity which leads to fast exchange of electrons between the enzyme and the electrode [22]. Carbon nanotubes and gold nanoparticles have high surface to volume ratio and strong electrical properties which facilitate the capacity of enzyme loading onto electron surface and amplify the signal. Nafion has also attracted much attention in biosensor applications due to its excellent thermal stability, biocompatibility, antifouling property as well as high mechanical strength. Additionally, nafion can effectively solubilize CNTs which help in fabrication of biosensors having both the efficient electrocatalytic property of CNTs and antifouling action of nafion films [23-24]. Chitosan (a biopolymer) has also been extensively used in biosensor fabrication owing to their hydrophilic nature, easy availability, high permeability, easy to modify, high mechanical strength, film-forming ability, low cost and non-toxicity [25]. To circumvent the use of additional redox mediators, the application of DET exhibiting hemoproteins and other enzymes which have the ability to transfer electrons directly towards the electrode opens new opportunities in the designing of biosensors and biofuel cells [26]. Hemoproteins are a huge class of proteins which have iron ions containing heme groups demonstrating unique oxidation/reduction properties suitable for DET. The majority of enzymes exhibiting DET towards the electrode have recognized intrinsic electron transfer pathways partly depending upon action of metal-coordinated complexes including heme-c, copper and iron-sulphur. Peroxidase was the first heme-c containing enzyme which was reported to transfer electrons efficiently to carbon [27-30] and gold based electrode [31]. Several DET-able heme-c based peroxidases including horseradish peroxidase [32-34], microperoxidase-11 (MP-11) [35] and microperoxidase-8 [28] have been applied in the field of biosensorics and bioelectronics. In health care sector, colossal potential of nanoparticles, DET-able enzymes and CNTs has enhanced scientific fervor towards development of biosensors for marketable accomplishments. In future, the utilization of biofuel cells as energy supplying source in the fabrication of biosensors will be promising [28].

In our research, we aspired to fabricate a new sensor having qualities like low cost, rapid response, good stability and reusability for alcohol detection. Alcohol oxidase and horseradish peroxidase were used to construct the bienzymic biosensor. AOX was covalently bound to PVC surface and

HRP, c-MWCNTs, AuNPs, nafion and chitosan were incorporated together onto Au electrode surface to construct a working electrode. Ethanol was oxidized by AOX and released H_2O_2 was further reduced by HRP to generate current. The combination of gold nanoparticles based working electrode and PVC immobilized enzyme for alcohol quantification represents the innovation of this work. This encourages replacement of working electrode on decay without loss of immobilized enzyme. In case of leaching out and denaturation of enzyme, re-use of working electrode can be done with a new enzyme immobilized beaker.

2. Experimental

2.1 Chemicals and reagents

Benzamidine, c-MWCNTs (ID 4-8nm, length 0.1-10 μM), sepharose 2B column, methylene chloride, chitosan (CHIT), NaN_3, polyethylene glycol, $HAuCl_4$ (0.01%), $AgNO_3$, nafion (5 % *w/v* in isopropanol), tween 60 from Merck, HRP (0.5 U/mg) from SRL, PVC beaker from local market and methanol, NH_4OH, H_2SO_4, Tris-HCl, HNO_3, acetic acid, $(NH_4)_2SO_4$, trisodium citrate, ABTS, glutaraldehyde from Himedia were used.

2.2 Instruments and Equipments

A potentiostat/galvanostat (PARSTAT 4000), FTIR (Varian 7000), Rotatory incubator shaker (HICON), UV-1800 UV-Vis Spectrophotometer, Water bath (SunRon), Refrigerator (LG), Magnetic stirrer (HICON), Deep freezer (Voltas), Digital pH meter (EUTECH), Microwave oven (LG) and Refrigerated centrifuge (SIGMA). SEM and TEM were done at AIRF, JNU, New-Delhi for surface morphology.

2.3 Revival and growth of Pichia pastoris (MTCC 34)

The yeast was obtained from IMTECH, Chandigarh, India. The revival of the lyophilized yeast strain was done by scraping off few cells from sample and streaking them on plated YPD (yeast extract, peptone, dextrose) media. UV-Vis spectrophotometer was used to assess the growth of yeast by examining optical density at 600 nm.

2.4 Enzyme extraction and purification

The extraction and purification of enzyme was done as method illustrated by Gvodev et al. [36] with minor changes. After growth of cells, centrifugation was done at 12,000 × g for 30 min and 0.02 M phosphate-citrate buffer was used to wash them twice. 0.01 mM benzamidine, 0.02% NaN_3, 0.05% tween 60 was added to the cell suspension and lysed with 1.2% (*w/v*) methylene chloride [37]. In cell-free solution, 0.1 M NH_4OH was added to adjust pH to 8 and later in 30% mixture (pH 7), $(NH_4)_2SO_4$ was added. Again centrifugation of mixture was done at the 12,000 × g for 40 min. $(NH_4)_2SO_4$ was added to the supernatant upto 60% of saturation and kept intact for 2 hrs at 5˚ C. Centrifugation of the resulting fraction was done for another time at 12,000 rpm for 15 min and obtained precipitates were then mixed in 0.01 M phosphate-citrate buffer. Ultrafiltration was done to separate the precipitates from salts and then 0.1 mM benzamidine, 0.02% NaN_3, 8-10% polyethylene glycol were supplemented to solution and stored. The resulting enzyme crystals were then collected via centrifugation at 12,000 rpm for 20 min and then suspended in buffer. Analytical centrifugation, gel filtration (sepharose 2B) followed by SDS PAGE was done for purifying crude alcohol oxidase.

2.5 Enzyme assay and protein estimation

The enzyme activity was determined by measuring the color generated from H_2O_2 in a coupled reaction using ABTS and HRP [38]. 0.1 mL AOX solution (purified) was dissolved in 0.01 mL HRP solution, 0.1 mL methanol, 2.8 mL ABTS solution and 0.01 mL potassium phosphate buffer. Then mixture was incubated for 50 min at 35˚ C. Reactions involved were as follows:

$$Methanol + O_2 \xrightarrow{AOX} Formaldehyde + H_2O_2$$

$$H_2O_2 + ABTS_{(Red.)} \xrightarrow{HRP} 2\,H_2O + ABTS_{(Ox.)}$$

AOX oxidizes methanol and produces formaldehyde and H_2O_2. Then HRP reduces H_2O_2 into H_2O by utilizing ABTS as electron donor, resulting in a green soluble end product. The spectrophotometer was used at 420 nm to measure the color produced. Then at $\lambda_{420\,nm}$, an increase in absorbance was observed due to production of H_2O_2 which indicated the enzyme activity. Lowry method was used for determining total protein concentration of dissolved enzyme using BSA as standard protein [39].

2.6 Enzyme immobilization on PVC beaker

The method explained by Hooda et al. was used for covalently immobilizing AOX onto PVC surface [19]. Firstly, nicks were introduced in the long vinyl polymer chains of PVC surface by treating it with a mixture of H_2SO_4 and HNO_3. Then 1.25% (*w/v*) glutaraldehyde in 0.05 M sodium phosphate buffer was used to incubate the beaker for 8 hr at 35˚ C. Glutaraldehyde reacts with free vinyl chains of PVC sheet to form -C=CH- bond. Then enzyme was immobilized on this activated PVC surface by incubating with 5.5 mL alcohol oxidase mixed in 50 mM sodium phosphate buffer at 4˚ C for 36 hr in dark. Then $–NH_2$ group present on enzyme surface covalently attached to –CHO group of glutaraldehyde via Schiff-base formation. Buffer was used to rinse the surface of beaker to remove unbound enzyme. Figure 1 illustrates the steps involved in AOX immobilization onto PVC beaker. Until use, beaker was kept in 0.1 M sodium phosphate buffer at 4˚ C. AOX immobilization was verified by SEM.

2.7 Immobilized enzyme assay

The similar procedure as illustrated for its native form was followed for immobilized AOX assay, omitting free enzyme with 0.1 mL of reaction buffer. During incubation, continuous stirring was done. After incubation, 0.01 mL HRP, 0.1 mL methanol solution, 2.8 mL ABTS solution and 0.01 mL potassium phosphate buffer was added to beaker and incubation was done for 50 min at 35˚ C to develop color. The spectrophotometer was used to measure the developed color at $\lambda_{420\ nm}$.

2.8 Synthesis of AuNPs and their characterization

AuNPs were prepared using method of Gole and Murphy (2004) with modifications [40]. 200 ml of $HAuCl_4$ (0.01%) was then heated at boiling point and continuously stirred followed by addition of sodium citrate (1%). The color of the solution turned to wine red within 2-3 min. Further, it was kept at room temperature for cooling and then stored at 4º C till further use. TEM of resultant AuNPs was done to confirm their shape and size.

2.9 Working electrode fabrication

Alumina slurry was used to rub bare Au electrode and rinsed with water prior to coating. Ultrasonication of Au electrode was done in ethanol. Thereafter rinsing of electrode was done two more times with deionized water and then dried. About 6 mg of c-MWCNTs were suspended in 600 µl of 5% Nf and sonicated for 40 min. 5 µl of the resulted homogeneous c-MWCNT-Nf

solution was added dropwise to Au electrode surface and dried. 0.4 g of CHIT flakes were dissolved in 40 mL of 1% acetic acid and stirred continuously. About 20 mg of AuNPs were dissolved in chitosan solution and stirred for 1 hr on magnetic stirrer. Sonication was done for 2 hr to get a homogeneous mixture. AuNPs/CHIT biopolymer matrix was electrodeposited on c-MWCNT/Nf/Au electrode surface using cyclic voltammetry at potential range of -0.75 to 1.2 V) and then dried. The resulting electrode was rinsed and dried again. Then AuNPs/CHIT/c-MWCNT/Nf/Au electrode was suspended in 2 ml of HRP solution (0.5 U/ml) for 24 hrs undisturbed to fabricate enzyme electrode. Finally working electrode HRP/AuNPs/CHIT/c-MWCNT/Nf/Au was washed with 0.1 M Tris-HCl buffer to remove traces of unconfined enzyme and stored in a refrigerator at 4 ˚C.

2.10 Biosensor assemblage and electroanalytical measurements

The assembly of sensor included AOX immobilized PVC reaction beaker accommodating HRP/AuNPs/CHIT/c-MWCNT/Nf/Au electrode, a reference electrode (Ag/AgCl) and an auxiliary electrode (Pt wire) connected to a potentiostat. The graphic representation of assembly has been shown in Figure 2. Cyclic voltammetric measurements were recorded between -0.70 V to +2.0 V at 50 mV/s (scan rate) at 35ºC. The optimum conditions were deliberated for the working of fabricated sensor.

2.11 Optimization of experimental parameters

The analytical recovery, accuracy, precision, minimum detection limit as well as linearity of the proposed sensor were evaluated. To attain optimal conditions for ethanol quantification, pH was changed from 4 to 8 at regular interval of 0.5 utilizing sodium acetate buffer and sodium phosphate buffer. Similarly, the determination of time of reaction and optimal temperature was done by incubating the solution at various time intervals (1-20 s) and temperatures (5-70˚ C). Various concentrations of ethanol (0.1-50 mM) were used to evaluate the effect of substrate quantity on current response. The values were correlated with standard graph to obtain LOD and linear working range. The storage stability was investigated by for 2 months by storing the reaction beaker at 4˚ C in 0.1 M sodium phosphate buffer. Some common substances present in real samples for e.g. urea, glucose, lactic acid, ascorbic acid and uric acid were examined for any interfering effects on ethanol detection.

3. Results and discussion

3.1 AOX purification from Pichia pastoris

The crude enzyme was extracted from *Pichia pastoris* culture which showed an activity of 0.87 U/ml (Table 1). Crude enzyme (AOX) was subjected to ammonium sulphate precipitation (0-80%), followed by Sephadex G-200 and DEAE- Sepharose 2B ion exchange chromatography for purification. The ammonium sulphate precipitation of crude enzyme resulted in 5.4-fold purification with 69.88% yield. The dissolved ammonium sulphate precipitate was further subjected to Sephadex G-200 column resulting in five peaks of enzyme activity (Figure 3). Four minor peaks comprised of fractions 13 to 17, 17 to 21, 30 to 34 and 35 to 37 respectively showed considerable activity of enzyme. The major peak comprised of fractions 22 to 30 showed maximum activity. Similarly five peaks were obtained for protein content. Maximum protein was obtained at a peak between 23 to 29 fractions, whereas four minor peaks were also observed for protein from 14 to 17, 17 to 21, 31 to 35 and 35 to 37 fractions. These active fractions from Sephadex G-200 were pooled, which showed overall 33.08 fold purification with 18.58% yield. The active fractions from Sephadex G-200 were collected and pooled. The pooled samples were subjected to DEAE-Sepharose 2B ion exchange chromatography, it resulted into three minor peaks and one major peak of enzyme activity. Fractions 7 to 9, 16 to 18 and 20 to 22 comprised of minor peaks, while the major peak was found in fractions numbering from 12 to 15. Maximum protein was also obtained in a major peak at fractions between 12 to 15 and minor peaks in 7 to 9, 16 to 18 and 20 to 22 fractions were also noted (Figure 4). The active fractions which showed high specific activity from DEAE-Sepharose 2B were collected and were treated as purified enzyme. DEAE-Sepharose 2B chromatography finally resulted in 39.37 fold purification with 17.93% yield and showed specific activity of 60.12 U/mg (Table 1).

3.2 Evidence for AOX immobilization on PVC beaker

AOX was covalently immobilized on PVC beaker with 65.25% of its initial activity and 0.40 mg/cm^2 conjugation yield. A uniform polymeric layer was seen in the SEM of bare surface of PVC beaker (Figure 5a) and globular beaded structure was observed in SEM of enzyme immobilized PVC surface (Figure 5b). It was evident from this change in surface morphology that enzyme was evenly packed within membrane.

3.3 Characterization of AuNPs

AuNPs were synthesized by method of by Gole and Murphy (2004) with some modification. UV visible spectroscopy and TEM were employed to characterize synthesized nanoparticles. UV/Vis spectra (Figure 6a) confirmed the synthesis of AuNPs by displaying absorption maxima at 526 nm. TEM analysis of AuNPs (Figure 6b) confirmed their spherical shape and average size in the range of 20-30 nm.

3.4 Electrochemical impedence spectroscopy (EIS) study

The different layers are formed during the fabrication of biosensor, as a result changes were observed in the impedence of the surface of electrode. Hence, EIS offers the valuable details regarding validation of these changes. The immobilization of HRP on Au electrode surface was confirmed through this technique. The Nyquist plot (Figure 7) displayed R_{CT} values of bare Au electrode, c-MWCNT/Nf/AuE, CHIT/AuNPs/c-MWCNT/Nf/AuE, HRP/CHIT/AuNPs/c-MWCNT/Nf/AuE in 6mM $K_3Fe(CN)_6/K_4Fe(CN)_6$ as 0.6 kΩ, 1.6 kΩ, 1.65 kΩ, 2.66 kΩ respectively. However an increase in R_{CT} value was observed with subsequent immobilization of HRP assigned to the reason that most biological molecules, including enzyme, have poor electrical conductivity at low frequencies. Hence it specified the binding of enzyme molecules on CHIT/AuNPs/c-MWCNT/Nf/AuE surface.

3.5 Cyclic voltammetric study of AOX and HRP based alcohol biosensor

The CV was performed for evaluating the electrochemical studies of AuNPs based working electrode (Figure 8). Bare Au electrode illustrated no clear peaks (curve a). AuNPs based working electrode displayed redox peaks at -0.25 V and -0.37 V (curve b). Later, biosensor was completely assembled by immobilizing AOX on PVC surface. The redox peaks (curve c) of generated assembly were nearly comparable to that of curve b, although high peak currents were observed. At the bioelectrode assembly, potential of redox couple was found to be -0.30 V, as estimated from formula $[(E_{pa}+E_{pc})/2]$ where E_{pa} represents anodic peak potential and E_{pc} represents cathodic peak potential. In earlier reports of direct electron transport process of HRP (Fe^{III}/Fe^{II}) [41], this potential was found to be similar. When ethanol was added, cathodic peak current was noticeably higher than anodic peak current verifying the redox potential of HRP (curve d). Ethanol was oxidized by the immobilized AOX to produce H_2O_2 which was then biocatalytically reduced by

HRP. As a result, HRP (Ox) was formed. Further DET mechanism was involved in electrocatalytic reduction of HRP (Ox) to HRP (Red) on electrode surface.

$$CH_3CH_2OH + O_2 \xrightarrow{AOX} CH_3CHO + H_2O_2$$

$$HRP\ (Red) + H_2O_2 \rightarrow HRP\ (Ox) + 2H_2O$$

$$HRP\ (Ox) + 2\,e^- + 2H^+ \xrightarrow{Electrode} HRP\ (Red)$$

3.6 Evaluation of fabricated biosensor

The bioelectrode responded optimally at pH 7.5 and temperature 35˚ C. The declination in the stability of enzyme was observed when deviated from the physiological temperature and pH [42]. The biosensor displayed optimal response within 12 s, which is shorter as compared to early reported sensors (Figure 9). When ethanol concentration was raised in range of 0.01 mM-42mM, linear increase in magnitude of cathodic current was observed but response was steady after 42mM (Figure 10). The current biosensor exhibited broad linear range of 0.01 mM-42mM and LOD of 0.0001 μM under optimal conditions.

3.7 Interference study and stability

To check the operational stability of sensor, 15 consecutive measurements were taken with 42 mM ethanol for duration of 8 hr. The current response was steady upto end and sensor retained about 90% of its initial activity. Reproducibility was predicted by examining the biosensor response to different ethanol concentrations at three bioelectrodes constructed similarly. The repeatability of sensor was confirmed when results showed ~1% relative standard deviation with acceptable reproducibility. The storage stability was examined by carrying out response measurements regularly after every 5 days. After 5 weeks, the sensor retained ~90% of its original response when kept in 0.02 M sodium phosphate buffer at 4˚ C. When sensor was regularly used for 80 times within 6 months, it lost half of its initial activity. The role of some interfering agents such as lactic acid, glucose, uric acid, urea and ascorbic acid was studied during ethanol detection at -0.35 V. Each interferent was separately exposed to analyte in ratio of 1:1 and then biosensor response was observed. The selectivity coefficient (SC) was ~1 for every interferent as estimated by following formulae:

$$SC = I_{c+i} / I_c$$

I_c represents response for ethanol in absence of interferent

I_{c+i} represents response for ethanol in presence of interferent

The current biosensor displayed tolerable anti-interferent ability and no considerable effect was noticed due to presence of these interferents.

3.8 Analysis of commercial samples

At -0.35 V, multiple standard addition procedure was utilized to estimate ethanol concentration ethanol (mg/ml) in four commercial samples of beer. Ethanol content in the samples I, II, III and IV was found to be 0.34±0.016, 0.54±0.013, 0.52±0.017 and 0.52±0.022 respectively. Similarly, the ethanol concentration in the same samples was also determined using ethanol assay kit which displayed results as 0.36±0.015 (I), 0.55±0.018 (II), 0.56±0.020 (III) and 0.49±0.018 (IV). The two separate methods showed noticeably similar results with correlation of 0.98 and no significant differences were observed (Figure 11). Therefore, reliability of the sensor was proved for quantitative analysis of commercial samples.

4. Conclusion

A novel sensor has been developed for ethanol detection by immobilizing HRP onto working electrode and AOX on PVC beaker. AuNPs and c-MWCNTs helped in the facilitation of direct electron exchange between electrode and HRP. At physiological pH, enzyme immobilized on PVC surface showed excellent electrocatalytic behavior. The application of PVC as an idyllic support in the current biosensor resulted in repeated utilization, storage stability as well as enhanced analytical performance. The fabricated biosensor displayed improved operational stability, minimum LOD and linear response range towards the substrate when compared with the early reported biosensors. The sensor responds within a short time period of 12 s in optimal conditions. As a good correlation was found between the presented biosensor and standard analytical methods, it can be extensively utilized in alcohol industries as well as healthcare areas.

Disclosure Statement

The authors report no potential conflict of interest.

References

[1] Yildiz HB, Toppare L. Biosensing approach for alcohol determination using immobilized alcohol oxidase. Biosens Bioelectron. 2006; 21:2306-2310.

[2] Santos AS, Pereira AC, Duran N, Kubota LT. Amperometric biosensor for ethanol based on co-immobilization of alcohol dehydrogenase and Meldola's Blue on multi-wall carbon nanotube. Electrochim Acta. 2006; 52:215-220.

[3] Azevedo AM, Prazeres DMF, Cabral JMS. Ethanol biosensors based on alcohol oxidase. Biosens Bioelectron. 2005; 21:235-247.

[4] Patel NG, Meier S, Cammann K, Chemnitius GC. Screen-printed biosensors using different alcohol oxidases. Sens Actuators B: Chem. 2001; 75:101–110.

[5] Svensson K, Bülow L, Kriz D, Krook M. Investigation and evaluation of a method for determination of ethanol with the SIRE Biosensor P100, using alcohol dehydrogenase as recognition element. Biosens Bioelectron. 2005; 21:705-711.

[6] Santos AS, Freire RS, Kubota LT. Highly Stable Amperometric Biosensor for Ethanol Based on Meldola' s Blue Adsorbed on Silica Gel Modified with Niobium Oxide. J Electroanal Chem. 2003; 547:135–142.

[7] Hooda V, Kumar V, Gahlaut A, Hooda V. Alcohol quantification: recent insights into amperometric enzyme biosensors. Artif Cells Nanomed Biotechnol. 2018; 46:398-410.

[8] Carelli D, Centonze A, De Giglio M, Quinto M, Zambonin PG. An interference-free first generation alcohol biosensor based on a gold electrode modified by an overoxidised non-conducting polypyrrole film. Anal Chim Acta. 2006; 565:27-35.

[9] Goswami P, Chinnadayyala SS, Chakraborty M, Kumar AK, Kakoti A. An overview on alcohol oxidases and their potential applications. Appl Microbiol Biotechnol. 2013; 97:4259-4275.

[10] Chinnadayyala SR, Kakoti A, Santhosh M, Goswami P. A novel ampero-metric alcohol biosensor developed in a 3rd generation bioelectrode platform using peroxidase coupled ferrocene activated alcohol oxidase as biorecognition system. Biosens Bioelectron. 2014; 55: 120-126.

[11] Tanriverdi S, Tuncagil S, Toppare L. A new amperometric alcohol oxidase biosensor based on conducting polymer of (4, 7-dithien-2-yl-2, 1, 3-benzothiadiazole). J Macromol Sci. 2012; 49:185-190.

[12] Wen G, Zhang Y, Shuang S, Dong C, Choi MM. Application of a biosensor for monitoring of ethanol. Biosens Bioelectron. 2007; 23:121-129.

[13] Gahlaut A, Dahiya M, Dhull R, Dilbaghi N. Fabrication of Nafion/HRP-SWCNT/MWCNT-ZnO based alcohol biosensor: diagnostics for forensic analysis. Int J Chem Anal Sci. 2014; 5:15-20.

[14] Das M, Barbora L, Das P, Goswami P. Biofuel cell for generating power from methanol substrate using alcohol oxidase bioanode and air-breathed laccase biocathode. Biosens Bioelectron. 2014; 59:184-191.

[15] Gorton L, Csöregi E, Domínguez E, Emnéus J, Jönsson-Pettersson G, Marko-Varga G, Persson B. Selective detection in flow analysis based on the combination of immobilsed enzymes and chemically modified electrodes. Anal Chim Acta. 1991; 250:203-248.

[16] Costa Rama E, Biscay J, González García MB, Julio Reviejo A, Pingarrón Carrazón JM, Costa García A. Comparative study of different alcohol sensors based on Screen-Printed Carbon Electrodes. Anal Chim Acta. 2012; 728:69-76.

[17] Moralesa A, Céspedesb F, Martínez-Fàbregasc E, Aligretc S. Ethanol amperometric biosensor based on an alcohol oxidase-graphite-polymer biocomposite. Electrochim Acta. 1998; 43:3575-3579.

[18] Chauhan N, Preeti, Pinky, Pundir CS. Covalent immobilization of uricase inside a plastic vial for uric acid determination in serum and urine. Anal Sci. 2014; 30:501-6.

[19] Hooda V, Gahlaut A, Kumar H, Pundir CS. Biosensor based on enzyme coupled PVC reaction cell for electrochemical measurement of serum total cholesterol. Sens Actuators B: Chem. 2009; 136:235-241.

[20] Pundir CS, Chauhan NS, Bhambhi M. Activation of polyvinyl chloride sheet surface for covalent immobilization of oxalate oxidase and its evaluation as inert support in urinary oxalate determination. Anal Biochem. 2008; 374:272-277.

[21] Pundir CS, Devi R, Narang J, Singh S, Nehra J, Chaudhry S. Fabrication of an amperometric xanthine biosensor based on polyvinylchloride membrane. J Food Biochem. 2011; 36:21-27.

[22] Antisari MV, Marazzi R, Krsmanovic R. Synthesis of multiwall carbon nanotubes by electric arc discharge in liquid environments. Carbon. 2003; 41:2393-2401.

[23] Wang J, Musameh M, Lin Y. Solubilization of Carbon Nanotubes by Nafion toward the Preparation of Amperometric Biosensors. J Am Chem Soc. 2003; 125:2408-2409.

[24] Fan ZH, Harrison DJ. Permeability of Glucose and Other Neutral Species through Reca st Perfluorosulfonated Ionomer Films. Anal Chem. 1992; 64:1304-1311.

[25] Inamdar NN, Mourya V. Chitosan and Low Molecular Weight Chitosan: Biological and Biomedical Applications. Adv Biomat Biodev. 2014; 1:183-242.

[26] Ramanavicius A, Ramanaviciene A. Hemoproteins in design of biofuel cells. Fuel cells 2009; 9:25-36.

[27] Ramanavicius A, Kausaite A, Ramanaviciene A. Biofuel cell based on direct bioelectrocatalysis. Biosens. Bioelectron. 2005; 20: 1962-1967.

[28] Ramanavicius A, Kausaite A, Ramanaviciene A. Enzymatic biofuel cell based on anode and cathode powered by ethanol. Biosens. Bioelectron. 2008; 24: 761-766.

[29] Wang M, Zhao F, Liu Y, Dong S. Direct electrochemistry of microperoxidase at Pt microelectrodes modified with carbon nanotubes. Biosens. Bioelectron. 2005; 21: 159-166.

[30] Yaropolov AI, Malovik V, Varfolomeev SD, Berezin IV. Electroreduction of hydrogen peroxide on an electrode with immobilized peroxidase. Dokl. Akad. Nauk. SSSR 1979, 249, 1399.

[31] Ruzgas T, Gaigalas A, Gorton L. Diffusionless electron transfer of microperoxidase11 on gold electrodes. J. Electroanal. Chem. 1999; 469:123-133.

[32] Katz E, Willner I, Kotlyar AB. A non-compartmentalized glucose-O_2 biofuel cell by bioengineered electrode surfaces. J. Electroanal. Chem. 1999; 479: 64-68.

[33] Pizzariello A, Stred'ansky M, Miertuš S. A glucose/hydrogen peroxide biofuel cell that uses oxidase and peroxidase as catalysts by composite bulk-modified bioelectrodes based on a solid binding matrix. Bioelectrochem. 2002; 56:99-105.

[34] Ernst A, Makowski O, Kowalewska B, Miecznikowski K, Kulesza PJ. Hybrid bioelectrocatalyst for hydrogen peroxide reduction: immobilization of enzyme within organic-inorganic film of structured Prussian Blue and PEDOT. Bioelectrochem. 2007; 71: 23-28.

[35] Willner I, Arad G, Katz E. A biofuel cell based on pyrroloquinoline quinine and microperoxidase-11 monolayer functionalized electrodes. Bioelectrochem. Bioenerg. 1998; 44: 209-214.

[36] Gvozdev AR, Tukhvatullin IA, Gvozdev RI. Purification and properties of alcohol oxidase from *Pichia putida*. Biochemistry (Moscow). 2010; 75:242-248.

[37] Hopkins TR. Red absorbing combination of alcohol oxidase and an azide compound. United State Patent, No. 4430427. 1984.

[38] Harrison JR. Large scale process for the purification of alcohol oxidase. United State Patent, No. 4956290. 1990.

[39] Kemp GD, Dickinson FM, Ratledge C. Inducible long chain alcohol oxidase from alkane-grown *Candida tropicalis*. Appl Microbiol Biotechnol. 1988; 29:370-374.

[40] Gole A, Murphy CJ. Seed-mediated synthesis of gold nanorods: Role of size and nature of the seed. Chemistry of Materials. 2004; 16:3633-3640.

[41] Xu Q, Mao C, Liu NN, Zhu JJ, Sheng J. Direct electrochemistry of horseradish peroxidase based on biocompatible carboxymethyl chitosan-gold nanoparticle nanocomposite. Biosens Bioelectron. 2006; 22:768-773.

[42] Kumar AK, Goswami P. Functional characterization of alcohol oxidases from *Aspergillus terreus* MTCC 6324. Appl Microbiol Biotechnol. 2006; 72:906-911.

[43] Barsan MM, Brett CMA. An alcohol oxidase biosensor using PNR redox mediator at carbon film electrode. Departamento de Quı mica, Universidade de Coimbra, 3004-535 Coimbra, Portugal. Talanta. 2008; 74:1505-1510.

[44] Hämmerle M, Hilgert K, Horn MA, Moos R. Analysis of volatile alcohols in apple juices by an electrochemical biosensor measuring in the headspace above the liquid. Sens Actuator B:Chem. 2011; 158:313-318.

Table 1: Purification data of AOX from *Pichia pastoris*

Fraction	Total volume (ml)	Protein (mg/ml)	Activity (Unit/ml)	Specific activity (Unit/mg)	Total protein (mg)	Total activity (Units)	Purification fold	% yield
Crude	150	1.085	0.87	0.0801	162.75	130.5	1	100
$(NH_4)_2SO_4$ precipitate	12	1.227	7.6	6.19	14.72	91.2	5.4	69.88
Sephadex G-200	15	0.061	1.617	36.50	0.91	24.52	33.08	18.58
DEAE-Sepharose 2B	14	0.053	1.672	60.12	0.74	23.50	39.37	17.93

Table 2: Comparison of various amperometric AOX based alcohol biosensors on basis of their performances.

Sr. No.	Transducer	Enzyme immobilization method	Minimum detection limit	Linearity	Response time	References
1.	Multi-walled carbon nanotube (MWCNT) modified glassy carbon electrode	Layer-by-layer technique	2.32 µM	5 µM -3000 µM	20 s	[10]
2.	PEDOT/TBTD/AOX electrode	Crosslinking	203.70 nA/mM	0.02 –1.7 mM	-	[11]
3.	Eggshell membrane electrode	Entrapment	30 µM	60 µM-0.80 mM	60 s	[12]
4.	Nafion/HRP-SWCNT/MWCNT-ZnO electrode	Crosslinking	10 µM	10 µM- 750 µM	10 s	[13]
5.	Au/MWCNT/Nf/ AOX/PEI bioelectrodes	Crosslinking	5 µM	8 µM -42 µM	55 s	[14]
6.	Graphite epoxy composite electrode (GECE)	Entrapment	-	2.5 µM -25 µM	70 s	[16]
7.	Graphite powder/an epoxy resin/AOX bicomposite electrode	Entrapment	-	0.5–29 mg/ml	-	[17]
8.	Carbon film/PNR/ AOX electrode	Crosslinking	29.7 µM	-	-	[43]
9.	Gas-diffusion working electrode	Crosslinking	9.9 µM	0.10 µM -30 mM	69 s	[44]
10.	AOX onto PVC surface and HRP/AuNPs/CHIT/c-MWCNT/Nf/Au electrode	Covalent bonding	0.0001 µM	0.01 mM-42 mM	12 s	Present work

AOX: Alcohol oxidase; HRP: horseradish peroxidase; MWCNT: multiwall carbon nanotube; Nf: Nafion; PEI: polyethylenimine; PEDOT: 3, 4-ethylenedio xythiophene; SWCNT: single wall carbon nanotube; TBTD: 4, 7-dithien-2-yl-2, 1, 3-benzothiadiazole.

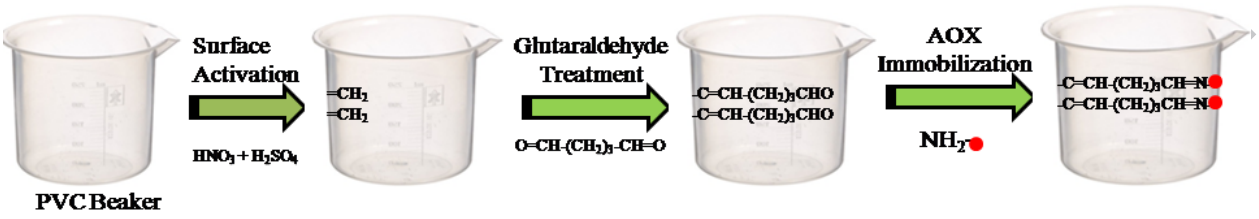

Figure 1: Mechanism involved in covalent immobilization of AOX on PVC surface

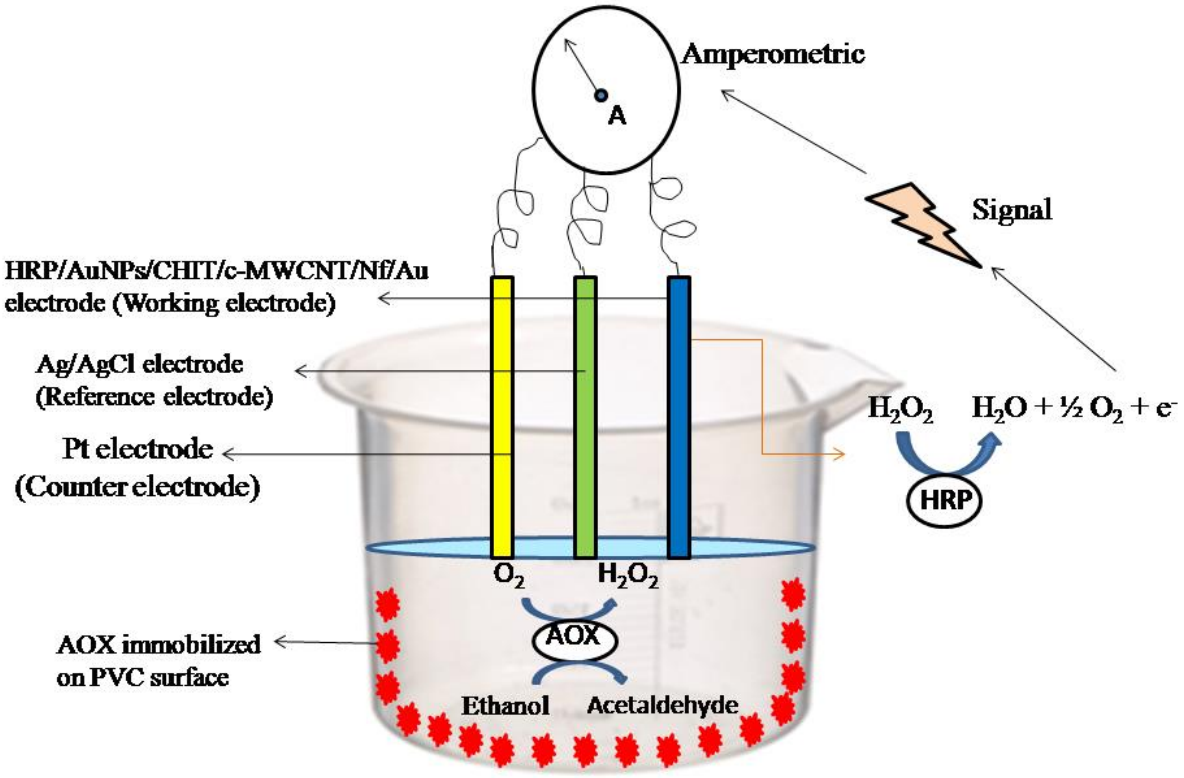

Figure 2: Assembly of AOX and HRP based amperometric alcohol biosensor

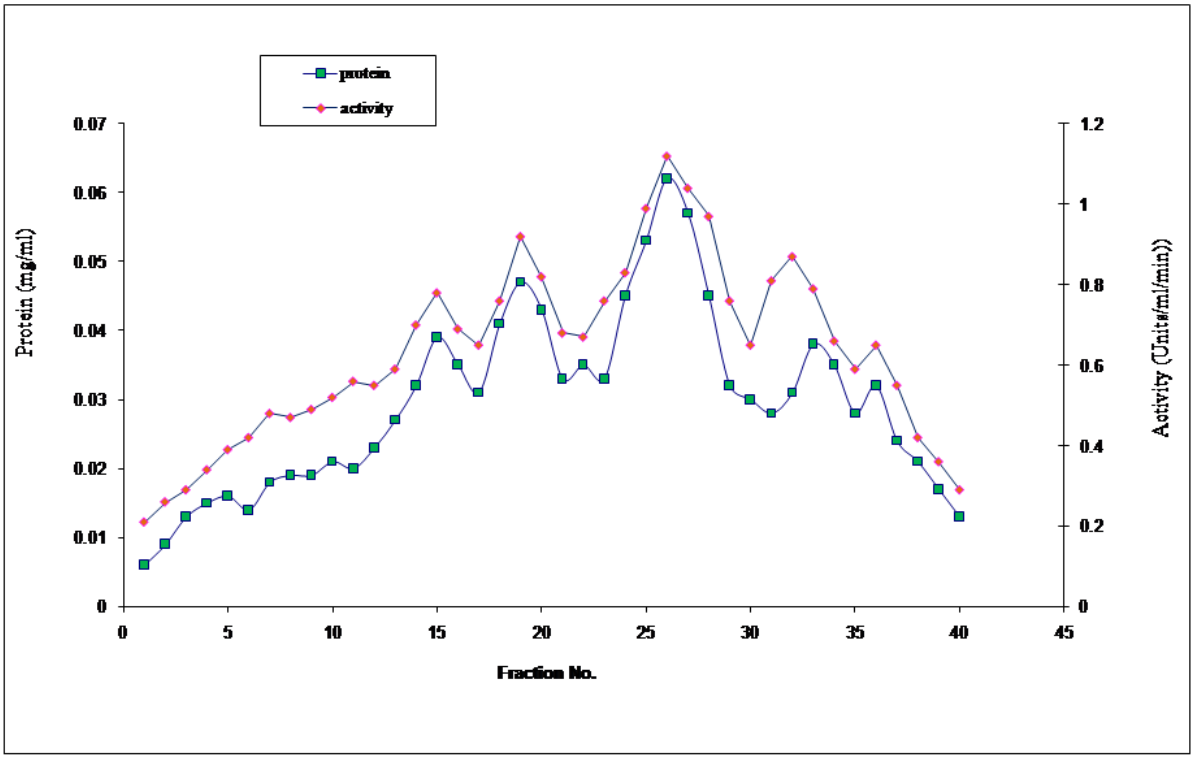

Figure 3: Gel filtration of crude fraction of AOX on Sephadex G-200 column chromatography

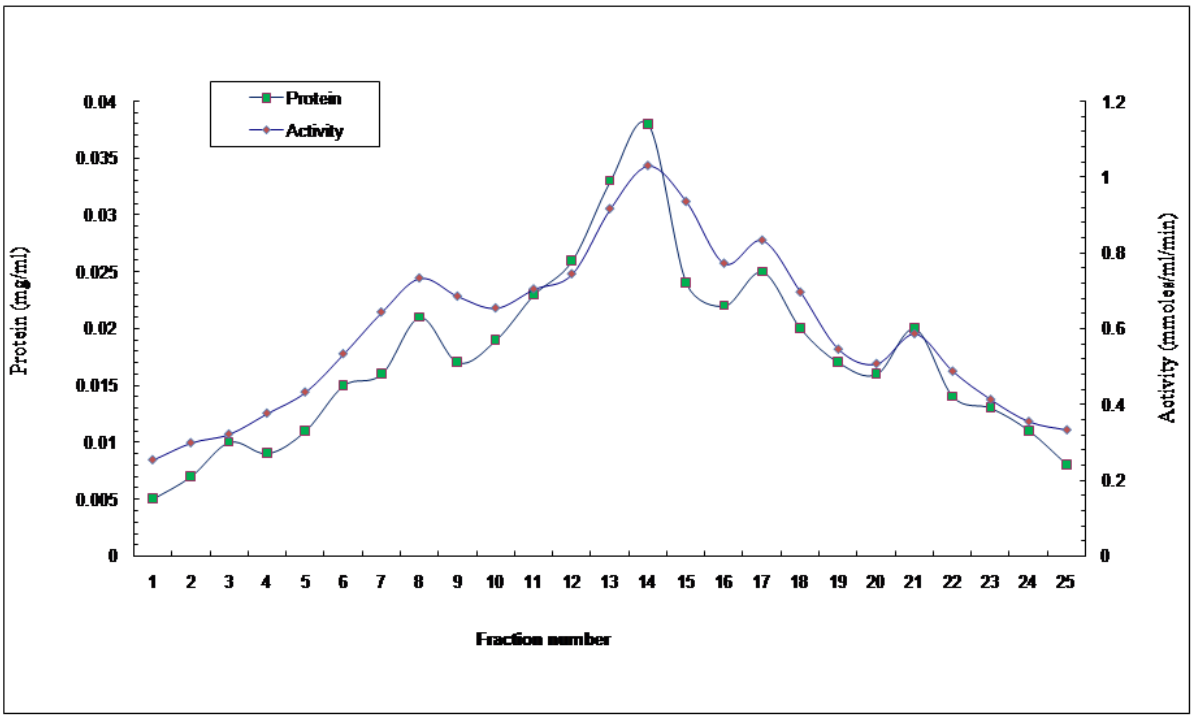

Figure 4: Ion-exchange chromatography of pooled fractions of Sephadex G-200 of AOX on DEAE-Sepharose 2B column

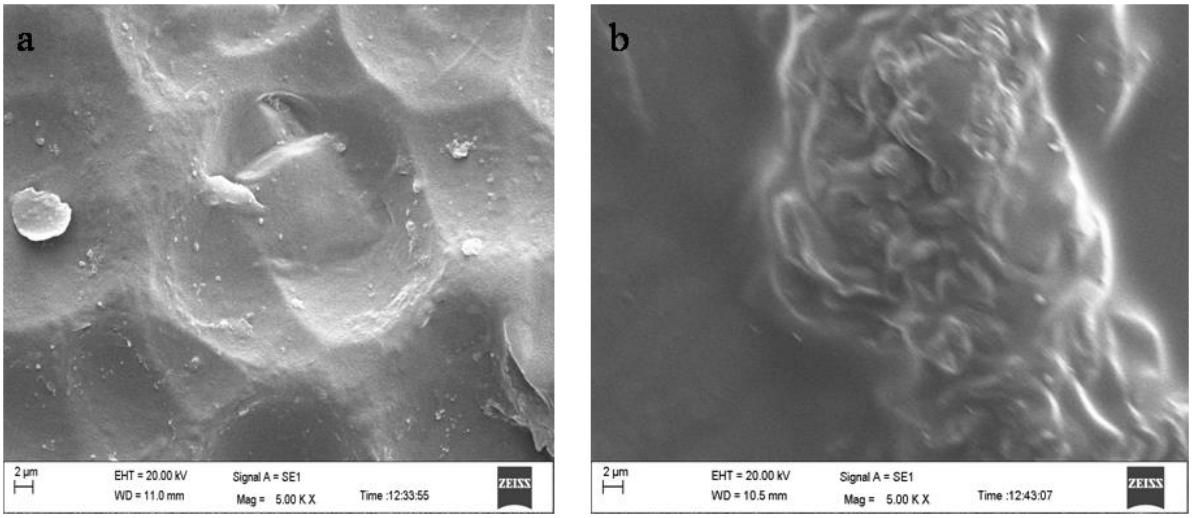

Figure 5: SEM images of (a) bare PVC surface (b) AOX immobilized PVC surface

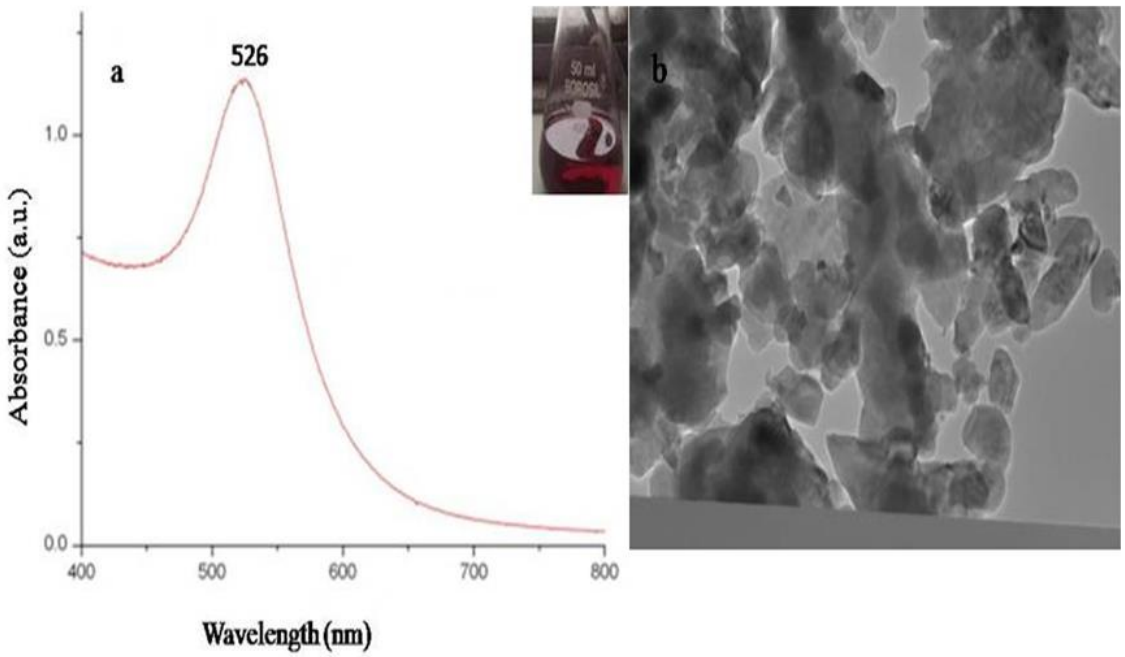

Figure 6: (a) UV-Visible spectrum of synthesized gold nanoparticles (b) TEM image of synthesized gold nanoparticles

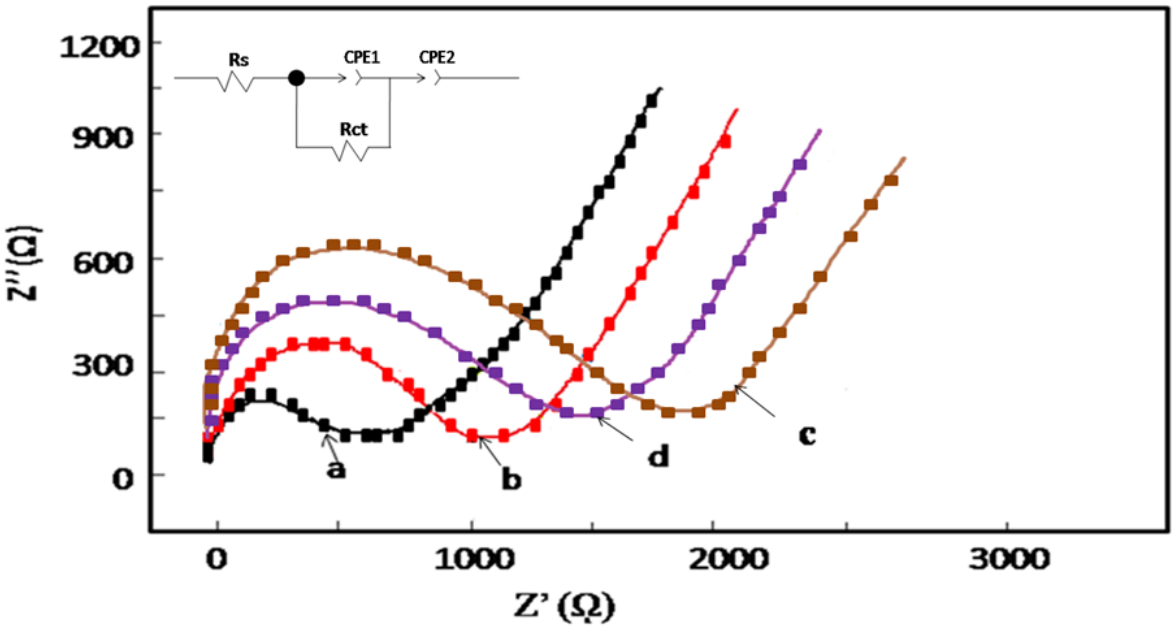

Figure 7: The Nyquist plot showing electrochemical impedence spectra (EIS) of (a) bare Au electrode (b) c-MWCNT/Nf/Au electrode (c) CHIT/AuNPs/c-MWCNT/Nf/Au electrode (d) HRP/ CHIT/AuNPs/c-MWCNT/Nf/Au electrode

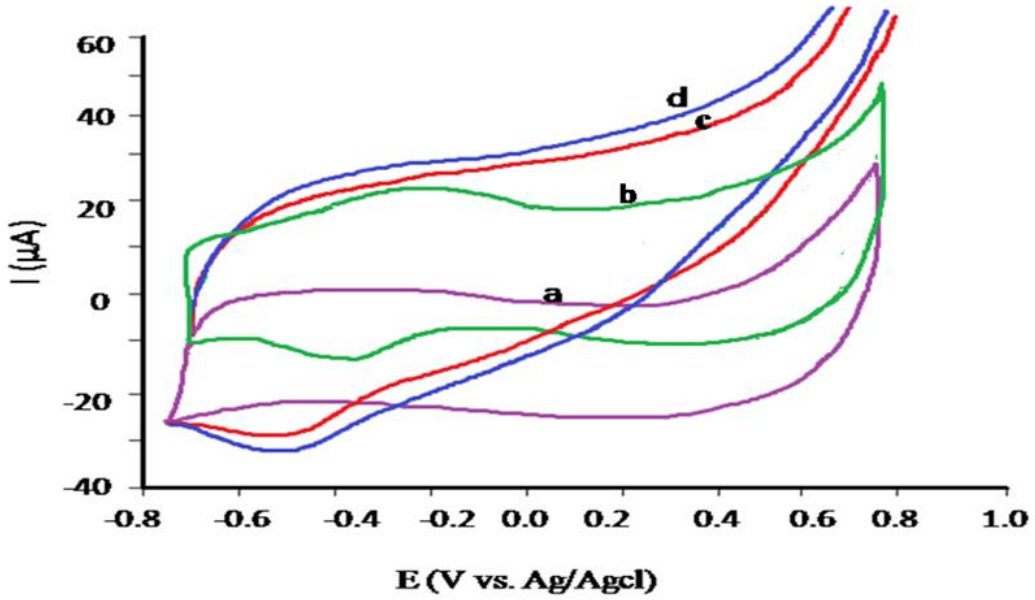

Figure 8: Cyclic voltammograms of (a) bare Au electrode (b) HRP/AuNPs/CHIT/c-MWCNT/Nf/Au electrode (c) complete assembly of biosensor without substrate (d) complete assembly of biosensor with substrate.

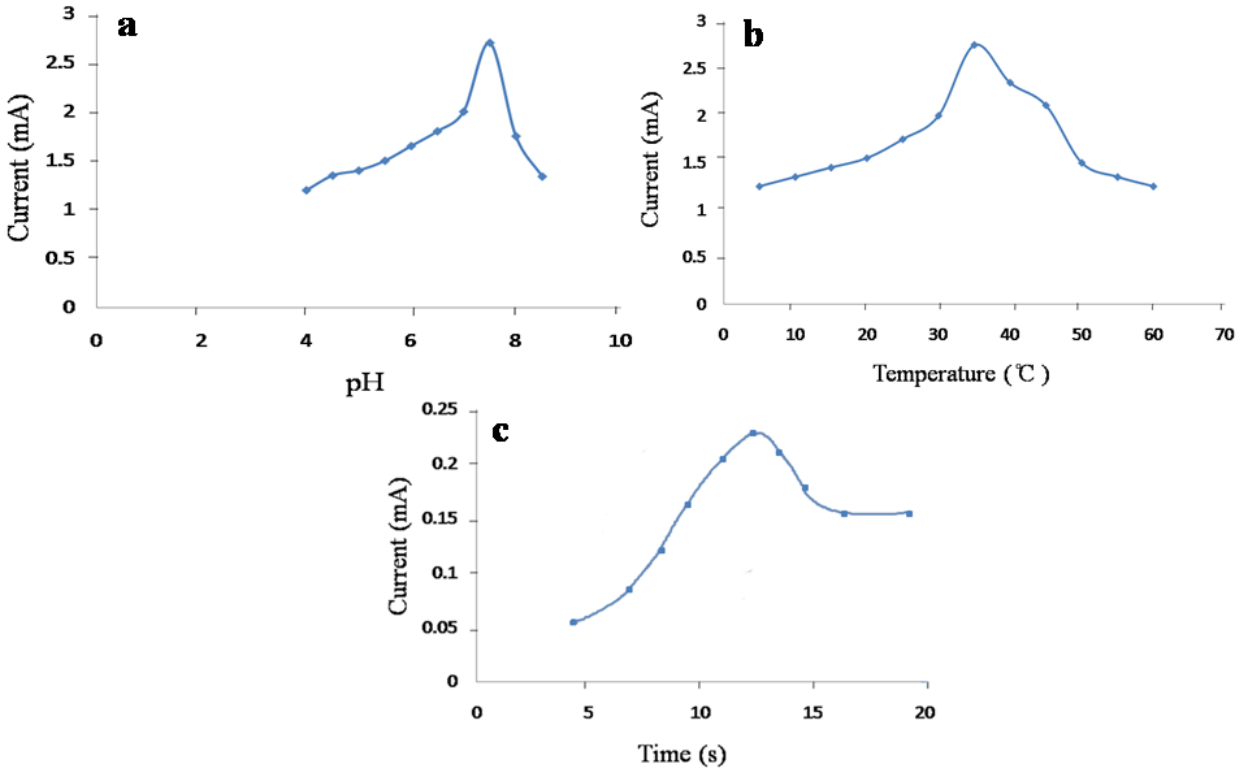

Figure 9: (a) Influence of pH on the current response of biosensor (b) Influence of temperature on the current response of biosensor (c) Influence of time on the current response of biosensor.

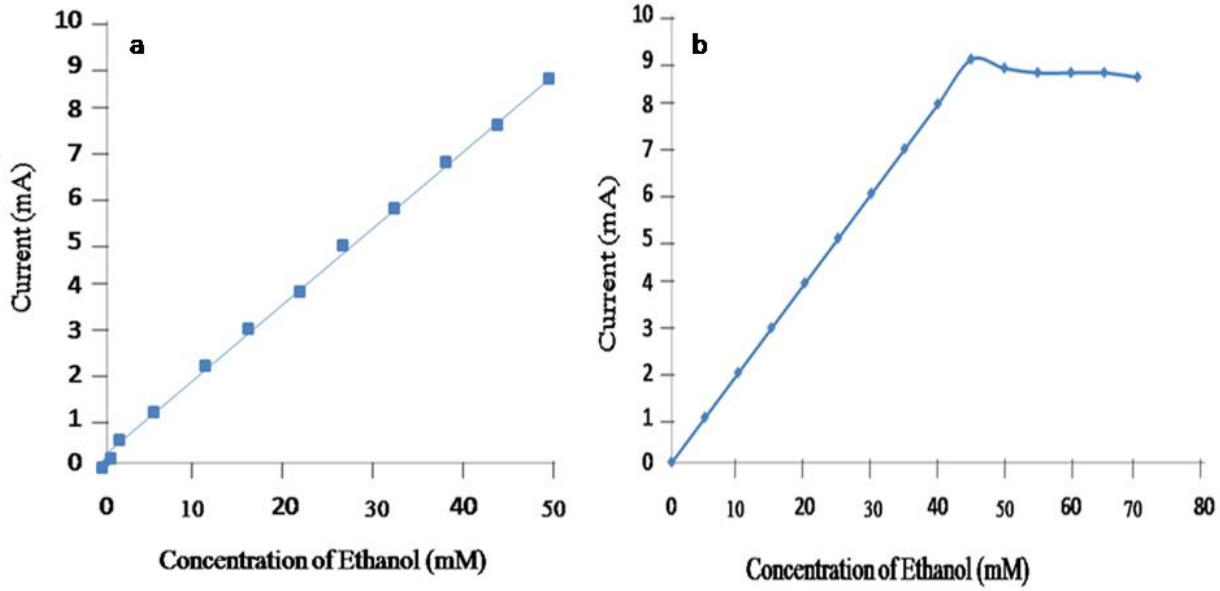

Figure 10: (a) Standard curve of ethanol by fabricated biosensor (b) Influence of ethanol concentrations on current response of biosensor.

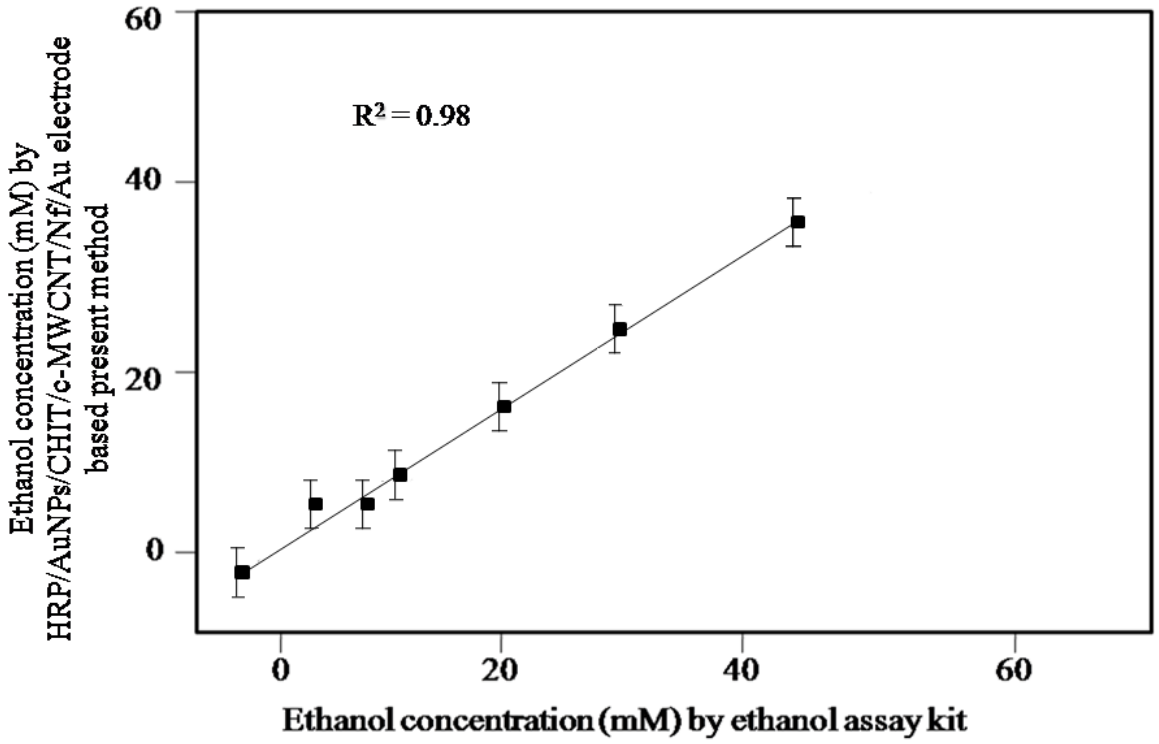

Figure 11: Correlation between ethanol level measured by ethanol assay kit (x-axis) and the present method (y-axis) employing HRP/AuNPs/CHIT/c-MWCNT/Nf/Au electrode